

**Kent State University**

---

**From the Selected Works of Peter Palffy-Muhoray**

---

April 1, 2002

# Three-Dimensional Dye Distribution in Photo-Oriented Liquid-Crystal Alignment Layers

S. Bardon

D. Coleman

N. A. Clark

T. Kosa, *Kent State University - Kent Campus*

H. Yuan, *Kent State University - Kent Campus*, et al.



Available at: [https://works.bepress.com/peter\\_palffy-muhoray/27/](https://works.bepress.com/peter_palffy-muhoray/27/)

## Three-dimensional dye distribution in photo-oriented liquid-crystal alignment layers

S. BARDON<sup>1</sup>, D. COLEMAN<sup>1</sup>, N. A. CLARK<sup>1</sup>, T. KOSA<sup>2</sup>,  
H. YUAN<sup>2</sup> and P. PALFFY-MUHORAY<sup>2</sup>

<sup>1</sup> *Condensed Matter Laboratory-Department of Physics, University of Colorado  
Boulder, CO 80309, USA*

<sup>2</sup> *Liquid Crystal Institute-Kent State University - Kent, OH 44242, USA*

(received 13 July 2001; accepted in final form 11 January 2002)

PACS. 61.30.Hn – Surface phenomena: alignment, anchoring, anchoring transitions, surface-induced layering, surface-induced ordering, wetting, prewetting transitions, and wetting transitions.

PACS. 61.30.Gd – Orientational order of liquid crystals; electric and magnetic field effects on order.

PACS. 42.70.Jk – Polymers and organics.

**Abstract.** – The three-dimensional optical anisotropy of photo-buffed dye-doped polymer films and the resulting orientation imparted to a liquid crystal in contact are probed using total internal reflection. Although the linearly polarized writing light generates a uniaxial distribution of dye molecules, the polymer films are biaxial, a result of symmetry breaking by the film surface.

Photo-induced anisotropy in dye-doped polymer films has great potential for application in optical storage [1] and in non-linear optics [2]. The dye molecules are attached to the polymer chain or dissolved in the polymer matrix and oriented using a writing beam. An important orientation mechanism is orientational hole burning via photo-induced *trans-cis* isomerization of the dye molecules [3]. Excitation of *trans*-isomers, with transition moment along the long axis, and orientational diffusion of the more mobile *cis*-isomers results in the depopulation of states with orientation along the pump beam polarization. Dye-doped polymer films also have the promise to replace mechanical buffing in the fabrication of LC displays [4]. It has been demonstrated that dye-doped Alignment Layers (ALs) allow the control of in-plane orientation of the liquid crystal with high spatial resolution [5] as well as tilted homogeneous anchoring of the LC [6].

In this letter, we use Total Internal Reflection (TIR) [7] to study both the dye distribution function in a thin polyimide film ( $t_{\text{AL}} = 210$  nm) and the resulting orientation of the LC molecules in the vicinity of this AL. The dye distribution is made anisotropic by illumination with green (514 nm) light. The dye molecules used in the experiment are elongated, with both the absorption dipole and the principal axis of the molecular polarizability tensor (corresponding to the largest polarizability) nearly parallel to the molecular long axis. Hereafter, the expression “dye distribution” refers to the distribution of this common axis. In the case

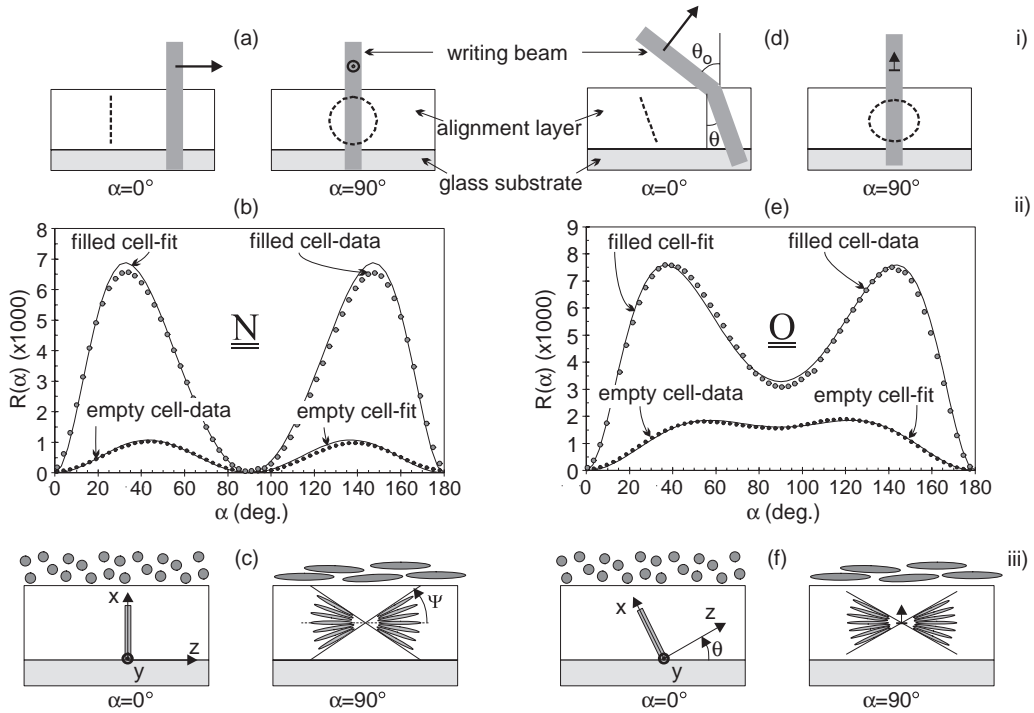


Fig. 1 – Sample N (*p*-polarized under normal incidence writing beam) and sample O (*p*-polarized under oblique incidence writing beam). i) Geometry of the writing process, the arrows represent the polarization direction of the beam,  $\alpha = 0$  corresponds the plane of incidence of the writing beam being coincident with plane of incidence of the probing beam. The dashed discs represent the contour of the dye distribution expected for an infinitely thick AL. ii) Experimental data (black dots for the empty cell and gray dots for the filled cell), fit of the empty cells (black lines), and calculated curves corresponding to the “numerical filling” process describing the filled cells (gray lines). iii) Sketch of the fan model used to describe the dye distribution: all the dye molecules are contained in the plane perpendicular to the writing polarization and the probability for the long axis of one molecule to be along any direction within the fan limited by  $\psi$  is constant and null outside the fan. Using this model, the fit of the empty cells allows us to determine  $\psi = 73^\circ$ ,  $\epsilon_t^{\text{AL}} = 2.96$  and  $\epsilon_l^{\text{AL}} = 3.10$ .

of a writing beam linearly polarized in the plane of incidence (*p*-polarized), the dye molecules are expected to have a uniaxial distribution with a disc-shaped surface of constant probability of orientation of the long molecular axis. (*cf.* dashed discs in fig. 1i)). The normal of the disc is expected to be along the direction of polarization of the write beam. Experimentally, we demonstrate that the dye distribution is biaxial, indicating that polymer film surfaces break the uniaxial symmetry; they thus play an important role in the orientation of the chromophores and consequently of the LC molecules. The anchoring of LC on these surfaces is planar, with the director perpendicular to the plane of incidence of the write beam, and, as expected by symmetry for this geometry, is without pretilt. Comparing the distribution function of the chromophores to the expected disc-like distribution provides insight into the effects of the polymer surfaces which may be crucial for understanding pretilt generation in these systems.

The samples consist of a layer of dye-doped polyimide spin-coated on high refractive index glass plates ( $n_g = 1.802$ ). The chromophores are azo-dye (Disperse Orange 3, Aldrich

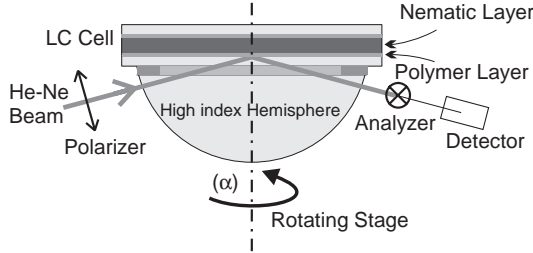


Fig. 2 – Setup for TIR study of the polymer layer and LC orientation near the glass surface via depolarization of the reflected He-Ne beam. The hemisphere and the bottom glass plate of the cell have the same high optical index ( $n_g = 1.802$ ) and we use index matching fluid to have a good contact between them.

Chemicals) dissolved in polyimide (PI2555, Du Pont). After imidizing at  $220^\circ\text{C}$  for 120 min, the number density of the dye is  $\sim 4 \times 10^{15}/\text{cm}^2$ ; using a profilometer, the thickness of the AL is found to be 210 nm. Photoalignment is carried out by irradiating the layer with plane polarized light from a CW  $\text{Ar}^+$  laser focussed to a  $40\ \mu\text{m}$  FWHM spot at 200 mW scanned at 4.5 mm/s. The total irradiated area is  $1\ \text{cm}^2$ . Cells are assembled after laser writing process with  $3\ \mu\text{m}$  polystyrene spacers. The cell is then filled with the room temperature nematic LC 5CB (*4'*-*n*-pentyl-4-cyanobiphenyl from BDH). We have performed experiments on 3 different samples. Sample M (Mechanically buffed) is rubbed with a buffing wheel (no optical alignment) and is used as a reference. Sample N is oriented by a normally incident *p*-polarized beam. Sample O is oriented by an obliquely incident ( $\theta_0 = 50^\circ$ , *cf.* fig. 1i) *p*-polarized beam.

The TIR setup is presented in fig. 2. A He-Ne laser beam ( $\lambda = 632\ \text{nm}$ ) polarized in the plane of incidence illuminates the LC cell through a high-refractive-index hemisphere at a fixed angle of incidence of  $75^\circ$ . The light is totally reflected at the glass/polymer/LC interface, and an evanescent wave (probe beam) propagates along the interface in the polymer and the LC. The penetration depth into the LC is  $\xi_{\text{LC}} \sim 100\ \text{nm}$ . Hereafter we will denote the depolarization ratio  $R(\alpha)$  as the ratio of the detected *s*-signal intensity to the incident *p*-wave intensity.  $R(\alpha)$ , measured as a function of  $\alpha$ , the angle between the buffing direction and the plane of incidence, gives information about the orientation of the dye in the polymer layer and of the LC close to the AL.  $R(\alpha)$  is periodic with period  $\pi$ , we therefore only present data corresponding to  $0 \leq \alpha \leq \pi$ . The experiments are carried out in two steps. First the signal from the empty cell is measured. Then the cell is filled with 5CB in the isotropic phase and cooled into the nematic phase where a second measurement is performed. The probe beam, because of its intensity and wavelength, has no effect on the orientation of the dye. The experimental data are fitted using numerical calculations using  $4 \times 4$  matrix methods [8, 9].

Figure 3 shows the measured results and the fit obtained with sample M filled and unfilled.  $R(\alpha)$  measured with the empty cell is similar to the ratio from a buffed sample without dye in the AL; the magnitude is comparable to experimental noise. The depolarization of the light due to the AL is therefore negligible, making the signal of the filled cell straightforward to analyze.  $R(\alpha)$  measured with the filled cell is typical of planar anchoring of the LC with the nematic director oriented along the rubbing direction and pretilted [7]. The two minima at

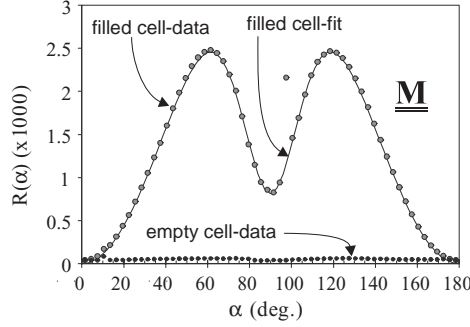


Fig. 3 – Experimental data and fit obtained on sample M (mechanical rubbing) filled and unfilled: (black dots) measurement on the empty cell; (gray dots) measurement on the filled cell; (gray line) fit of the filled cell with an isotropic AL and a homogeneous pretilted orientation of the LC having the nematic director along the rubbing direction. The fit allows us to determine  $n_{AL} = 1.734 \pm 0.002$ ,  $\beta = 4.7 \pm 0.2^\circ$  and  $\langle Q \rangle_{TIR} = Q_{bulk} \pm 0.1$ .

$\alpha = 0$  and  $\alpha = \pi/2$  correspond, respectively, to the LC being parallel (broad minimum) and perpendicular (narrow minimum) to the plane of incidence of the probe beam. For  $\alpha = \pi/2$ ,  $R(\alpha)$  (narrow minimum) is not equal to 0, showing that the LC director is tilted away from the AL by an angle ( $\beta$ ). Mechanical rubbing typically produces such LC alignment. Assuming a uniaxial distribution and a homogeneous nematic LC order parameter ( $Q$ ) throughout the cell, the maximum of  $R(\alpha)$ ,  $R_{MAX}$ , depends only on the optical index of the AL and its thickness  $t_{AL}$  through  $e^{-2\pi t_{AL} n_{AL}/\lambda}$ . The ratio  $R(\pi/2)/R_{MAX}$  depends only on the pretilt angle ( $\beta$ ). Therefore, the fitted curves are entirely determined by  $R_{MAX}$  and  $R(\pi/2)/R_{MAX}$ . Then, the abscissa of the two maxima provide a cross-check of the assumption of the homogeneity of the nematic order parameter and, along with  $R_{MAX} \sim Q^2$  provide a sensitive measurement of  $Q$  near the AL surface. Simulations give  $n_{AL} = 1.734 \pm 0.002$ ,  $\beta = 4.7 \pm 0.2^\circ$ . The bulk optical indices, and therefore the bulk nematic order parameter, were used everywhere ( $\langle Q \rangle_{TIR} = Q_{bulk} \pm 0.1$ , where  $\langle Q \rangle_{TIR}$  is the value of  $Q$  which describes the experimental data assuming that  $Q$  is constant). Qualitatively,  $\langle Q \rangle_{TIR}$  may be interpreted as the average of  $Q$  with  $e^{-2\pi z/\lambda}$  as a weight function. In the following, the value of  $n_{AL}$  is kept constant, and the birefringence,  $\delta n^{AL}$ , of the AL induced by the anisotropic distribution of the dye molecules is treated as a perturbation from this value. In the case of uniaxial distribution  $n_{AL}^{ord} = (n_{AL} - \delta n^{AL}/3)$  and  $n_{AL}^{ext} = (n_{AL} + 2\delta n^{AL}/3)$ .

Figure i) presents the experimental data and the numerical fits obtained with samples N and O. The  $R(\alpha)$  measured with the two empty cells are much larger than that of the rubbed cell and have the symmetry required by the system ( $C_{2,v}$ , with the rotation axis perpendicular to the cell plates and one of the mirror planes coinciding with the plane of incidence of the writing beam). Therefore,  $R(\alpha)$  data on samples N and O give information both on the dye and the LC distributions. Hereafter, we call buffing direction the intersection between the plane of incidence of the writing beam and the glass plates. Qualitatively, the signal of the empty cell N exhibits a minimum at  $\alpha = 0$  which is narrower than the minimum at  $\alpha = \pi/2$ . This indicates that  $n_{AL,z} < n_{AL,y}$ , which is opposite to what has been observed on sample M (filled). Moreover, when the writing beam is obliquely incident (sample O), the signature of tilt (non-zero minimum of  $R(\alpha)$ ) appears in the  $R(\alpha)$  curve of the empty cell at  $\alpha = \pi/2$ . From sample N, we know that the minimum at  $\alpha = \pi/2$  is broad. Therefore, the comparison of the two empty cell signals shows that the axis having the smaller refractive index ( $n_{AL,z}$ ) becomes

tilted away from the AL when the writing beam is obliquely incident. These observations are in accord with disc-like distribution for the dye because such a distribution would have a negative birefringence. However, it is not possible to fit our data using a uniaxial distribution for the dye.

In order to describe the dye distribution, we assume that all the dye molecules are contained in the plane perpendicular to the polarization of the write light in the polymer. For sample O, the tilt of this plane is deduced from Snell's law and is  $\theta = 26^\circ$ . The probability for a dye molecule to be along a given direction in this plane is denoted  $f(\varphi)$ , where  $\varphi = 0$  corresponds to the direction parallel to the glass plates. We further assume that  $f$  is periodic with period  $\pi$  and is even in  $\varphi$ . Then, the optic axes are along the normal to the plane containing the dye molecules ( $z$ , *cf.* fig. liii)), along  $\varphi = 0$  ( $y$ ) and  $\varphi = \pi/2$  ( $x$ ). The corresponding permittivity tensor is obtained by averaging the molecular permittivity tensor over  $f$  (eq. (1)). By decomposing  $f$  in a Fourier series, we obtain a simple expression for  $\epsilon$  (eq. (2)). Equation (2) shows that all the distributions having the same Fourier coefficient  $a_2$  are optically equivalent. Therefore, for the sake of simplicity, we will work with the fan model presented in fig. liii). This model corresponds to a function  $f$  that is constant for  $0 \leq \varphi \leq \psi$  and null for  $\psi \leq \varphi \leq \pi/2$ . In this case, the permittivity tensor (eq. (3)) depends only on  $\epsilon_1$  and  $\psi$  ( $\epsilon_t$  is given by  $(2\epsilon_t + \epsilon_1)/3 = n_{\text{AL}}^2$ ).

$$\begin{aligned}\epsilon_{xx} &= \epsilon_1 \langle \sin^2 \varphi \rangle_f + \epsilon_t \langle \cos^2 \varphi \rangle_f, \\ \epsilon_{yy} &= \epsilon_1 \langle \cos^2 \varphi \rangle_f + \epsilon_t \langle \sin^2 \varphi \rangle_f, \\ \epsilon_{zz} &= \epsilon_t,\end{aligned}\tag{1}$$

$$\begin{aligned}\epsilon_{xx} &= (\epsilon_1 + \epsilon_t)/2 - \Delta\epsilon a_2, \\ \epsilon_{yy} &= (\epsilon_1 + \epsilon_t)/2 + \Delta\epsilon a_2, \\ \epsilon_{zz} &= \epsilon_t,\end{aligned}\tag{2}$$

$$\begin{aligned}\epsilon_{xx} &= \frac{\epsilon_1 + \epsilon_t}{2} - \Delta\epsilon \frac{\cos \psi \sin \psi}{\psi}, \\ \epsilon_{yy} &= \frac{\epsilon_1 + \epsilon_t}{2} + \Delta\epsilon \frac{\cos \psi \sin \psi}{\psi}, \\ \epsilon_{zz} &= \epsilon_t,\end{aligned}\tag{3}$$

where  $\Delta\epsilon = (\epsilon_1 - \epsilon_t)/2$ ,  $a_2 = \int_0^{2\pi} f(\varphi) \cos(2\varphi) d\varphi$ .

The best fits of the two empty cell signals are presented in fig. lii) and give  $\psi = 73^\circ$ ,  $\epsilon_t = 2.96$  and  $\epsilon_1 = 3.10$  (corresponding to a birefringence  $\delta n_{\text{unx}}^{\text{AL}} = 0.04$  for the uniaxial case ( $\psi = 0$ )) in both cases, within experimental error. Results that strongly support our approach are as follows. Once  $\psi$  and  $\epsilon_1$  are determined as previously described, we can “numerically fill” the cell with the nematic planar aligned (no pretilt), with the director perpendicular to the buffing direction, and assuming that the nematic order parameter is constant and equal to its bulk value throughout the cell. The results of the corresponding calculations of the depolarized ratio for the filled cell (no fit) are presented in fig. lii) with the filled cell experimental data for samples N and O. We observe that the calculated and the experimental curves are in excellent agreement with no need for parameter adjustments (the discrepancy in the peak intensity for sample N is within the error in the determination of  $\psi$  and  $\epsilon_1$ ). Furthermore, simulations show that the TIR signal of the “numerically filled” cells depends strongly on  $\psi$ , making this observation meaningful. Therefore, a simple model containing only two adjustable parameters describes the four TIR curves presented in fig. 1.

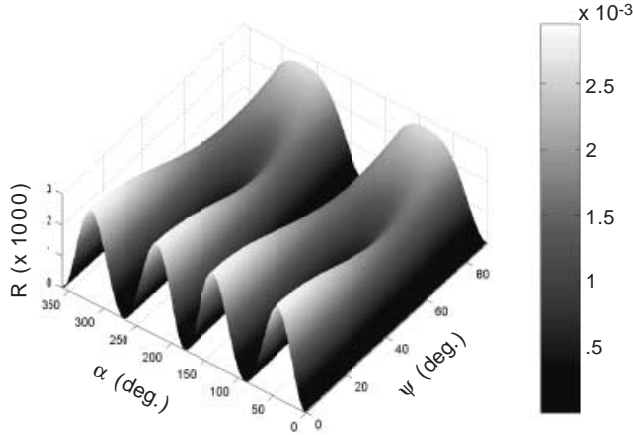


Fig. 4 – Simulation of the evolution of the TIR signal ( $R(\alpha)$ ) when the opening angle of fan distribution ( $\psi$ ) is increased. The plane of the fan is tilted by  $\theta = 26^\circ$  and  $\delta n_{\text{uniox}} = 0.04$ .

Figure 4 presents a simulation of the evolution of the TIR curve, for an empty cell, as the opening angle of the fan ( $\psi$ ) is increased. The plane of the fan is tilted by  $\theta = 26^\circ$  and  $\delta n_{\text{uniox}}^{\text{AL}} = 0.04$ .  $\psi = 0$  corresponds to a homogeneous planar distribution with the long axis of the dye molecules along  $\mathbf{y}$ .  $\psi = \pi/2$  corresponds to an uniaxial disc-like distribution. The main feature of this plot is the increase of the relative intensity of the minimum  $R(\pi/2)$  relative to  $R_{\text{MAX}}$  when  $\psi$  increases, accompanied by a significant displacement of the abscissa of  $R_{\text{MAX}}$ . This is due to a continuous increase of  $(n_{\text{AL},X} - n_{\text{AL},Z})$  from 0 for  $\psi = 0$  to  $(\epsilon_1 - \epsilon_t)^2/4$  for  $\psi = \pi/2$ . Therefore, we see how the biaxiality of the dye distribution, described via  $\psi$ , enters the model.  $\psi = 73^\circ$  corresponds to a biaxiality  $\delta n_{XY}^{\text{AL}} = 0.009$  (compared with  $\delta n_{YZ}^{\text{AL}} = 0.025$ ). The existence and the sign of the biaxiality are not model-dependent. However, several different distributions of the dye molecules may be used to describe our data (as shown by eq. (2)).

The observed biaxiality, interpreted in this letter as a distortion of the uniaxial disc distribution, arises from the effect of polymer surfaces on the orientation of the dye molecules. From our results, we conclude that these surfaces tend to increase the relative number of molecules parallel to the surface. Our data can also be described using a distribution which is not homogeneous throughout the polymer layer. For example, the addition at the polymer surfaces of a 15 nm thick interface-layer of planar aligned dye (parallel to the LC) to a non-distorted uniaxial disc-like distribution also fits our data. Since polymer surfaces have an effect on the dye distribution, the anchoring properties of a dye-doped AL will depend on the layer thickness, particularly in the case of thin layers. The generation of pretilt of the LC by using circularly polarized light [6] or “two steps” may depend sensitively on this factor.

\*\*\*

The authors would like to thank M. MEADOWS and J. E. MACLENNAN for stimulating discussions on this topic. This work was supported in part by the AFOSR under MURI grant no. F49620-17-1-0014, and the NSF under ALCOM grant no. 89-DMR20147 and MERSEC grant DMR9809555. One of us (SB) thanks Thomson-CSF for financial support.

## REFERENCES

- [1] TODOROV T., NIKOLOVA L. and TOMOVA N., *Appl. Opt.*, **23** (1984) 4309.
- [2] SEKKAT Z., PRÊTRE P., KNOESEN A., WOLKSEN W., LEE V. Y., MILLER R. D., WOOD J. and KNOLL W., *J. Opt. Soc. Am. B*, **15** (1998) 401.
- [3] BLINOV L. M., *J. Nonlin. Opt. Phys. Mat.*, **5** (1996) 165.
- [4] SHANNON P. J., GIBBONS W. M. and SHUN S. T., *Nature*, **368** (1994) 532.
- [5] GIBBONS W. M., KOSA T., SHANNON P. J., PALFFY-MUHORAY P. and SUN S. T., *Nature*, **377** (1995) 43.
- [6] LIM T. K., CHOI S. U. and PARK Y. I., *Jpn. J. Appl. Phys.*, **35** (1996) L1281.
- [7] XUE J.-Z., CLARK N. A. and MEADOWS M. R., *Appl. Phys. Lett.*, **53** (1988) 2397.
- [8] BERREMAN D. W., *Phys. Rev. Lett.*, **28** (1972) 1683.
- [9] YUAN H., W. E., KOSA T. and PALFFY-MUHORAY P., *SID 98 Digest*, (1998) 818.